

NOTES AND CORRESPONDENCE

On the Elevation Dependency of Present-day Climate and Future Change over Korea from a High Resolution Regional Climate Simulation

Eun-Soon IM

National Institute of Meteorological Research, Korea Meteorological Administration, Korea

and

Joong-Bae AHN

Department of Atmospheric Sciences, Pusan National University, Korea

(Manuscript received 4 March 2010, in final form 13 October 2010)

Abstract

This study investigates the elevation dependency of the present-day climate and future climate change in temperature and precipitation over Korea. A dynamically downscaled fine-scale climate simulation (20 km) shows reasonable agreement with two types of observations maintained by the Korea Meteorological Administration. The model exactly captures the strong relationship between the elevation and local climatology as seen in observed temperature and precipitation patterns. The behavior of the elevation dependency shown by the present-day climate simulation is also appeared in the climate change signal. The warming amplification is highly correlated with elevation. The warming is more pronounced at higher elevations than at lower elevations during winter, and maximum warming occurs at minimum temperature, showing an asymmetric response between minimum and maximum temperature. A noticeable differential rate of winter warming in response to the elevation can be explained by the snow-albedo feedback. Precipitation and snow changes also show the relevant topographical modulation under global warming. This study clearly demonstrates the importance of a refined topography for improving the accuracy of the local climatology and suitably reflecting the altitudinal distribution.

1. Introduction

Surface elevation is a key factor in modulating the temperature and precipitation change due to global warming (Fyfe and Flato 1999; Giorgi et al. 1997; Kim 2001; Kim et al. 2002; Im et al. 2010a). As a supporting fact, the most sensitive and vulnerable areas to

climate change are in mountainous regions, especially at high elevation sites (Beniston et al. 1997; Beniston 2003). A wide range of altitudinal variation on a mountain can give rise to a sharp gradient of vertical change in the temperature lapse rate (Barry 2008). This, in particular, can affect non-linear and threshold surface processes such as snow formation and melting, mostly tied to local snow-albedo feedback. Consequently, this characteristic leads to a pronounced spatial complexity of the climate change signal even within a short horizontal distance.

To deal with such a marked elevation dependency within the framework of modeling studies, explicitly

Corresponding author: Eun-Soon Im, National Institute of Meteorological Research, Korea Meteorological Administration, 460-18 Shindaebang-dong Dongjak-gu Seoul 156-720 Korea

E-mail: esim@korea.kr

©2011, Meteorological Society of Japan

representing the interactions between surface variables and the underlying topography is essential (Leung and Ghan 1999; Qian et al. 2009), thus fine-mesh experiments that suitably resolve complex topography are necessary. In spite of the recent rapid improvement in computing power, it is still difficult to simulate fine-scale climate change projections because climate change information should be based on long-term statistics (covering several decades to hundreds of years). This is one of the main reasons that intensive examinations of the characteristics of elevation dependency have been relatively limited, even though this issue is a critical factor in determining the local response to global warming (Giorgi et al. 1997).

As an attempt to accurately assess the impact of climate change over Korea, we performed a downscaling of the ECHAM5-MPI/OM global projection under the A1B emission scenario for the period 1971–2100 using the RegCM3 one-way double-nested system. The Korean peninsula appears to be a particularly representative region that can highlight the need for a high resolution modeling system because of its complicated geographical features (Im et al. 2006). Physically-based long-term (130-year) fine-scale (20 km) climate information is appropriate for analyzing the detailed structure of the elevation dependency of Korean climate change. In addition, the Korean territory is covered by a relatively dense observational network (in spite of the restrictions of high elevation sites), which makes it possible to estimate the first-order validation of the fine-scale structure of the nested model simulation. In the first part of the presentation of results (Section 3.1), we assess how well the model can capture the topographically induced signature of surface climate in relation to the elevation dependency against ASOS (Automated Surface Observing Systems) and Automatic Weather Stations (AWS) observations. We then consider the behavior of future climate change strongly constrained by topographical forcing (Section 3.2). Analysis is mostly centered on the temperature (mean, maximum, and minimum) and precipitation.

2. Model and observation

To produce fine-scale climate change information, focusing on the Korean peninsula and based on the fourth Assessment Report (AR4) of the Intergovernmental Panel on Climatic Change (IPCC 2007), a model chain composed of ECHAM5-MPI/OM and RegCM3 has been developed (Im et al. 2011). Simulations with the RegCM3 double-nested system used in this study have already been extensively analyzed and have demonstrated its applicability to the Korean region (Im et

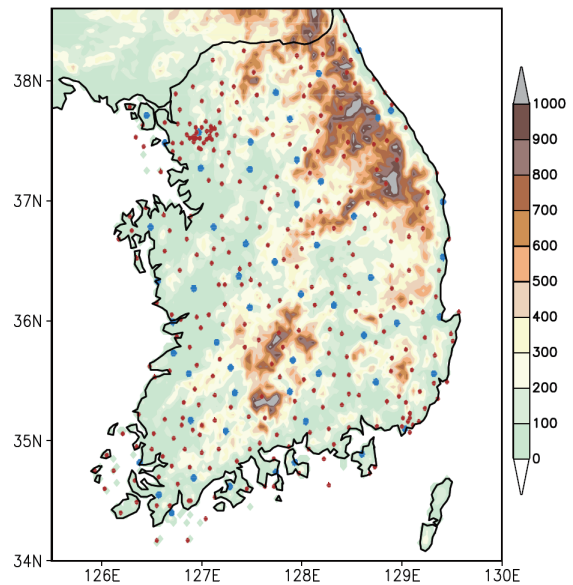


Fig. 1. Topography (m) and distribution of 57 ASOS (blue dot) and 295 AWS (red dot) used in analysis of observational data.

al. 2006, 2007b, 2011; Im and Kwon 2007). The ECHAM5/MPI-OM is a state-of-the-art coupled global climate model, which was used to conduct ensemble simulations for the IPCC AR4, and has been successfully downscaled over the European region (e.g., Hagemann et al. 2009). Moreover, the temperature and precipitation changes over East Asia (including the Korean peninsula) simulated by ECHAM5/MPI-OM are not markedly different from those of the 18 AOGCMs participating in the CMIP3 A1B projections (See Fig. 9 in Im et al. 2011). Therefore, even though this study is based on a single realization—one emission forcing (A1B, which lies in the middle range of the IPCC emission scenarios), one GCM (ECHAM5/MPI-OM) and one RCM (RegCM3), our results are built on firm ground. Both the global and regional climate models are described in detail by Im et al. (2006, 2011) and the references therein.

In our double-nested system, the mother domain covers East Asia at 60 km grid spacing, while the nested domain focuses on the South Korean peninsula at 20 km grid spacing (See Fig. 1 in Im et al. 2011). It is clearly shown that the representation of the mountain depends critically on the model resolution. The initial and time-dependent meteorological lateral boundary conditions for the mother domain simulation are interpolated at 6-hourly intervals from an ECHAM5/MPI-OM A1B sce-

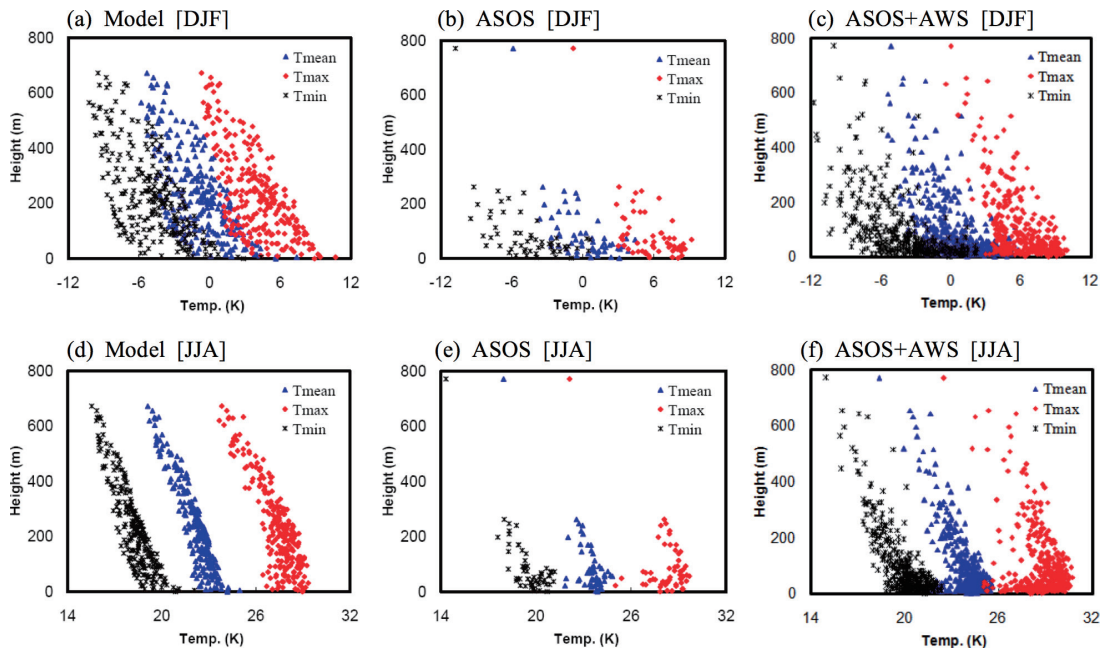


Fig. 2. Scatter plots of the altitudes of 248 model grid points (a and d), 57 ASOS (b and e) and 352 ASOS+AWS (c and f) against mean (T_{mean}), maximum (T_{max}) and minimum (T_{min}) temperature at the corresponding locations for the winter (upper panels) and summer (lower panels).

nario simulation. The integration spans 130 years, consisting of present-day conditions as a reference (covering the 30-year period 1971–2000) and future climate conditions (covering the 100-year period 2001–2100).

For the validation of the reference simulation (1971–2000), we first used climate observations from 57 stations with long-term time series and few missing data. Quality control of the data was maintained by the Korea Meteorological Administration (KMA) for the period from 1975 to 2004 throughout the southern part of Korea. Figure 1 shows the locations of the meteorological stations (blue dots, hereafter denoted as ASOS, Automated Surface Observing Systems) and topography. The ASOS serves as the KMA’s primary surface weather observing network. Although the selected 57 ASOS stations were located at both low and high elevations, most of the stations were situated below 300 m with one exceptional place (Daegwallyeong, 772.4 m). To overcome this limitation, we added 295 Automatic Weather Stations (red dots in Fig. 1, hereafter AWS) data to the period of 1997–2006 in addition to the ASOS data. The availability of the AWS data is relatively recent since the KMA has installed the AWS stations nationwide and intensively only since the mid-1990s. There are 464 AWS stations operating and data-

quality-controlled by KMA at the moment, but for this study, we selected only 295 AWS stations which had at least 300 daily observations per year for the entire period. Adding up ASOS and AWS stations, we have 352 locations relatively evenly distributed with 12.65 km of mean horizontal distance between stations. The mean, maximum, and minimum temperatures and precipitation from the inner nested domain of 20 km grid spacing (248 grid points) are compared to corresponding values from the 57 ASOS 30-year (1974–2005) data, as well as the 352 ASOS+AWS 10-year (1996–2006) data. The relatively high model resolution justifies the comparison between station data and grid point model data (Im et al. 2007a). Note that, since the climatology of the recent 10 years (352 ASOS+AWS) could be different from that of the 30-year (57 ASOS) climatology, this comparison is not intended to provide quantitatively accurate validation. It is, rather, aimed at investigating the qualitative behavior as a supplementary analysis.

3. Results

3.1 Validation of present-day climate simulation (1971–2000)

We begin our analysis with the seasonally (DJF and JJA) averaged 30-year climatology of mean, maximum,

Table 1. Summary of basic statistics derived from Figs. 2 and 3.

		Correlation		Mean		Standard Deviation	
		DJF	JJA	DJF	JJA	DJF	JJA
T_{mean}	Model	-0.68	-0.92	-0.86	22.16	2.42	1.07
	ASOS	-0.60	-0.79	0.15	23.43	2.19	0.98
	ASOS +AWS	-0.63	-0.77	-0.31	23.61	2.33	1.13
T_{max}	Model	-0.69	-0.85	4.02	27.36	2.35	1.20
	ASOS	-0.58	-0.49	5.73	28.22	2.02	1.27
	ASOS +AWS	-0.60	-0.43	5.23	28.21	1.86	1.29
T_{min}	Model	-0.64	-0.87	-4.94	18.24	2.63	1.09
	ASOS	-0.56	-0.80	-4.67	19.52	2.68	1.14
	ASOS +AWS	-0.60	-0.81	-4.91	19.73	3.01	1.37
Preci.	Model	0.36	0.60	2.11	9.48	0.44	1.33
	ASOS	0.10	0.31	1.03	7.86	0.26	1.05
	ASOS +AWS	-0.09	0.19	0.87	9.21	0.31	1.22

and minimum temperatures (hereafter referred to as T_{mean} , T_{max} , and T_{min}). Figure 2 shows the relationship between elevation and T_{mean} , T_{max} , and T_{min} for winter and summer. Note that both observational datasets and the model grid points do not have the same altitudinal distribution.

Compared to the ASOS data, the ASOS+AWS data shows a more widely scattered pattern, maintaining the fundamental structure found in the ASOS. The temperature decreases with height, showing different seasonal lapse rates, i.e., since the lapse rate of dry air is larger than that of moist air, the slopes in winter are steeper than summer slopes. Also the lapse rates of T_{max} are larger than those of T_{min} , possibly due to more moisture contained at daytime air mass. In spite of the discontinuity between approximately 300 m and 800 m, due to the absence of ASOS stations, the ASOS clearly shows elevation dependency. The values of the Daegwallyeong site (772.4 m) dotted at the upper parts of the figures (b and e) are lowest compared to those of other lower stations, which leads us to expect roughly linear decreases of temperature with altitude. The simulated temperature distributions match the observed ones reasonably well. The model exactly captures the overall seasonal dependence, with the dispersion being more spread in winter than in summer. One reason for the wide spread of tem-

perature in winter may be that the horizontal gradient of temperature is large in winter. Also captured are the seasonal mean values of T_{mean} , T_{max} , and T_{min} , although the model tends to underestimate temperature compared to observation (Table 1). The negative bias between the model and ASOS is larger than that between the model and ASOS+AWS, regardless of T_{mean} , T_{max} , and T_{min} . It is reasonable to guess from the above discussion that the larger discrepancy with ASOS could be attributed to the low density of high elevation ASOS stations. In order to estimate the elevation dependency quantitatively, we provide the correlation coefficients between temperatures and heights as well (Table 1). Consistently, with the scatter plots of Fig. 2, the model shows higher coefficients in all cases. Due to the sparse horizontal distribution and even absence of specific height ranges in the ASOS, and due to more complex terrain and surface states in real situations of ASOS+AWS, both observations show relatively low correlation coefficients against heights, compared to the model results. The observed coefficients are, however, still high enough to be statistically significant at the 95% confidence level.

Whereas the temperature shows strong elevation-dependent features in both seasons, the precipitation has rather weak and mixed behavior (Fig. 3). But it still shows systematic seasonal and altitudinal distributions.

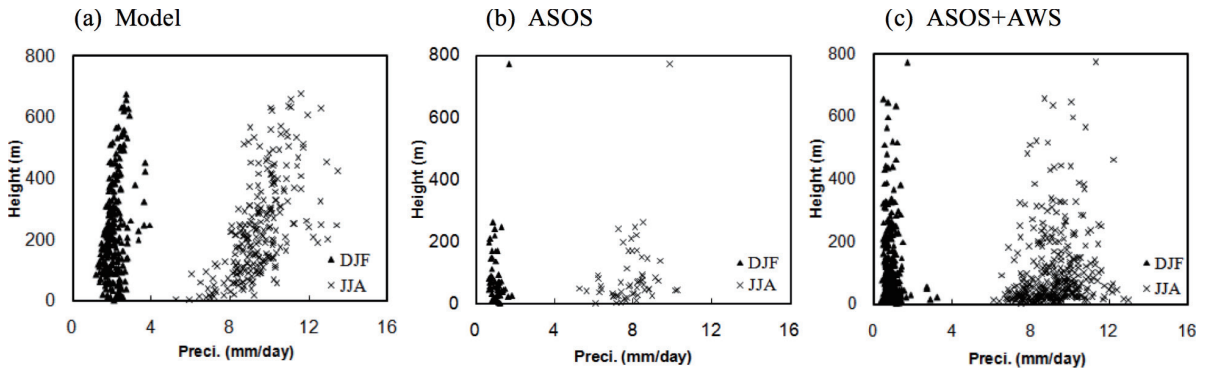


Fig. 3. Scatter plots of the altitudes of 248 model grid points (a), 57 ASOS (b) and 352 ASOS+AWS (c) against precipitation at the corresponding locations for the winter and summer.

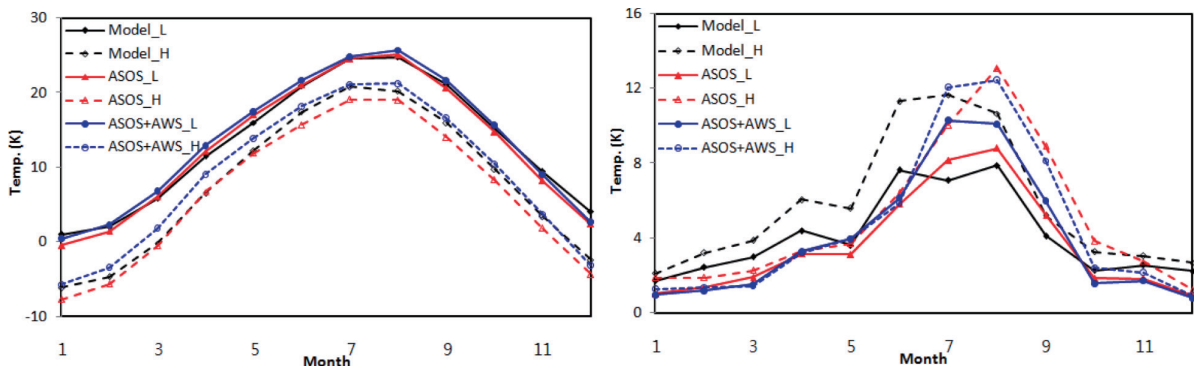


Fig. 4. Monthly variation of temperature (left) and precipitation (right) averaged over low and high elevation categories. Here, L and H denote the low ($0 < h < 50$) and high ($h > 600$) elevations, respectively.

For winter, no significant relationship between precipitation and elevation is found in both observations and simulation. It is rather uniform and slightly increasing in altitude. Despite the pronounced scatter of the data, it can be seen that the summer precipitation is dependent on the elevation, especially in the simulation. In fact, summer precipitation over Korea is affected by stochastic and relatively less predictable processes such as the occurrence of monsoon convective systems and tropical storms behind the topographic forcing (Im et al. 2006). Nevertheless, there is likely to be more precipitation at high-elevation sites than at lower sites. Due to the high concentration of data at the low level, the correlations derived from both observed data are less relevant. However, both coefficients (0.31 for ASOS and 0.19 for ASOS+AWS) are also statistically significant at the 95% confidence level.

To clearly demonstrate the elevation dependency of the seasonal evolution of temperature and precipitation,

we separately calculated the monthly variation in T_{mean} and precipitation for two elevation ranges, namely low and high levels (Fig. 4). The number of stations included in the low and high elevation categories (Low: $0 < h < 50$, High: $h > 600$) were different for both observations and the simulation (Low: Model = 22, ASOS = 26, ASOS + AWS = 153, High: Model = 8, ASOS = 1, ASOS + AWS = 4). Of course, one observation site (Daegwallyeong) of ASOS may not represent the general characteristics of the high elevation category. Furthermore, the selected period of ASOS+AWS is different from that of the simulation and ASOS (see Section 2. Model and Observation). Therefore, this comparison is necessarily limited in scope and aims to provide a semi-quantitative indication of the behavior.

Considering T_{mean} (left panel in Fig. 4), first of all, the model shows an excellent phase coherence with the observed monthly variation. The simulated values of the low elevation are, for the most part, close to both

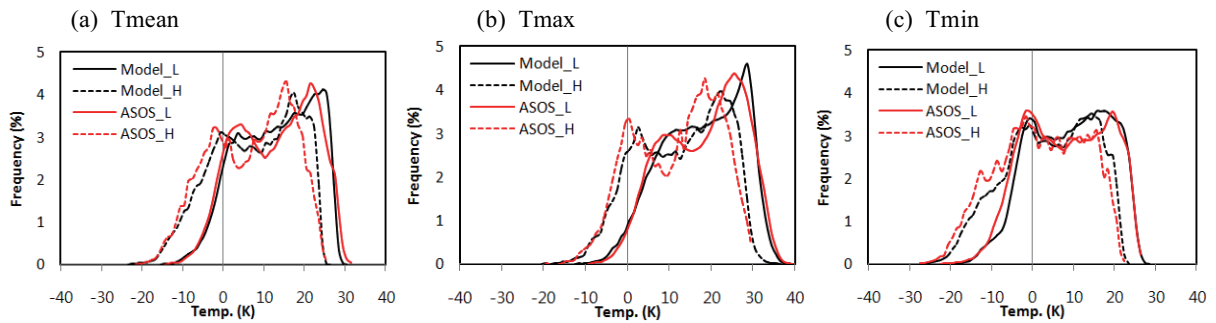


Fig. 5. Frequency distribution of daily T_{mean} , T_{max} , and T_{min} over low and high elevation categories. Here, L and H denote the low ($0 < h < 50$) and high ($h > 600$) elevations, respectively.

ASOS and ASOS+AWS values while the model systematically overestimates the high elevation temperatures (except for April) compared to ASOS values. This might be caused by the height difference. The average height of the 8 model grid points included in the high elevation category is lower than the height of the Daegwallyeong site. Except for several months, the model is in better agreement with ASOS+AWS. Similar behavior is also found for T_{max} and T_{min} (not shown). The increase in precipitation with elevation is also visible during the warm season (right panel in Fig. 4). It is difficult to assess the absolute comparison between the simulation and observations because they are not under the same conditions in terms of data period and the number of data used. However, the model and both observations consistently provide seemingly more enhanced precipitation over the higher elevations.

Due to the great variability and the complex interactions between orography and weather systems, it is very difficult to obtain a general relationship between precipitation and elevation. Although several previous studies found various dependencies of precipitation amounts on elevation, these studies are also accompanied with some caveats. For example, Sasaki and Kurihara (2008) show that precipitation generally increases with elevation from the non-hydrostatic regional climate simulation and station observational system over Japan, but their relationship becomes clear through appropriate classification of the area.

For a detailed analysis of the statistics regarding daily events, we present the frequency distribution of daily T_{mean} , T_{max} , and T_{min} for the low ($0 < h < 50$) and high ($h > 600$) elevations from 30-year simulation and ASOS data (Fig. 5). At the lower elevation, the shape of the annual distribution exhibits a bimodal structure reflecting the contributions of different distribution characteristics

for the cold season and the warm season. There is a noticeable difference in the shape of T_{max} and T_{min} distributions, such as a more asymmetric T_{max} distribution. At the higher elevation, the distribution pattern mostly manifests itself with a shift of the distribution towards lower values. In spite of some deficiencies in the central tendency (e.g., mean) and dispersion (e.g., standard deviation or variance) of the daily values, the model is able to depict the basic structure of each distribution realistically. By comparison, it is found that the low elevation results of the simulation agree better with observed patterns than the high elevation results. Again, it is attributed to the scarcity of stations at higher elevations in the ASOS data. As for the precipitation, it is difficult to derive a well-defined pattern from the frequency distribution of discontinuous daily events (not shown).

Indeed, the lack of sufficient stations throughout the various ranges of heights is a limitation of this study. Further work, based on high-quality fine-scale observational datasets, is needed to validate the detailed performance of the fine-mesh model experiment. Despite these caveats, Figures 2–5 indicate that the RegCM3-ECHAM5/MPI-OM model chain appears to produce reliable climate information, in terms of both temperature (T_{mean} , T_{max} , and T_{min}) and precipitation. The model captures different seasonal behavior in response to elevation dependencies of temperature and precipitation (except for winter precipitation). Observed patterns based on 57 ASOS and 352 ASOS+AWS are in line with the results of simulation, although the degree of dependencies between variables and elevation are weakened due to the unevenness of vertical data distribution. Given this validation of the model performance, we turn our attention to the elevation dependency of the climate change signal over Korea from the nested domain simulation.

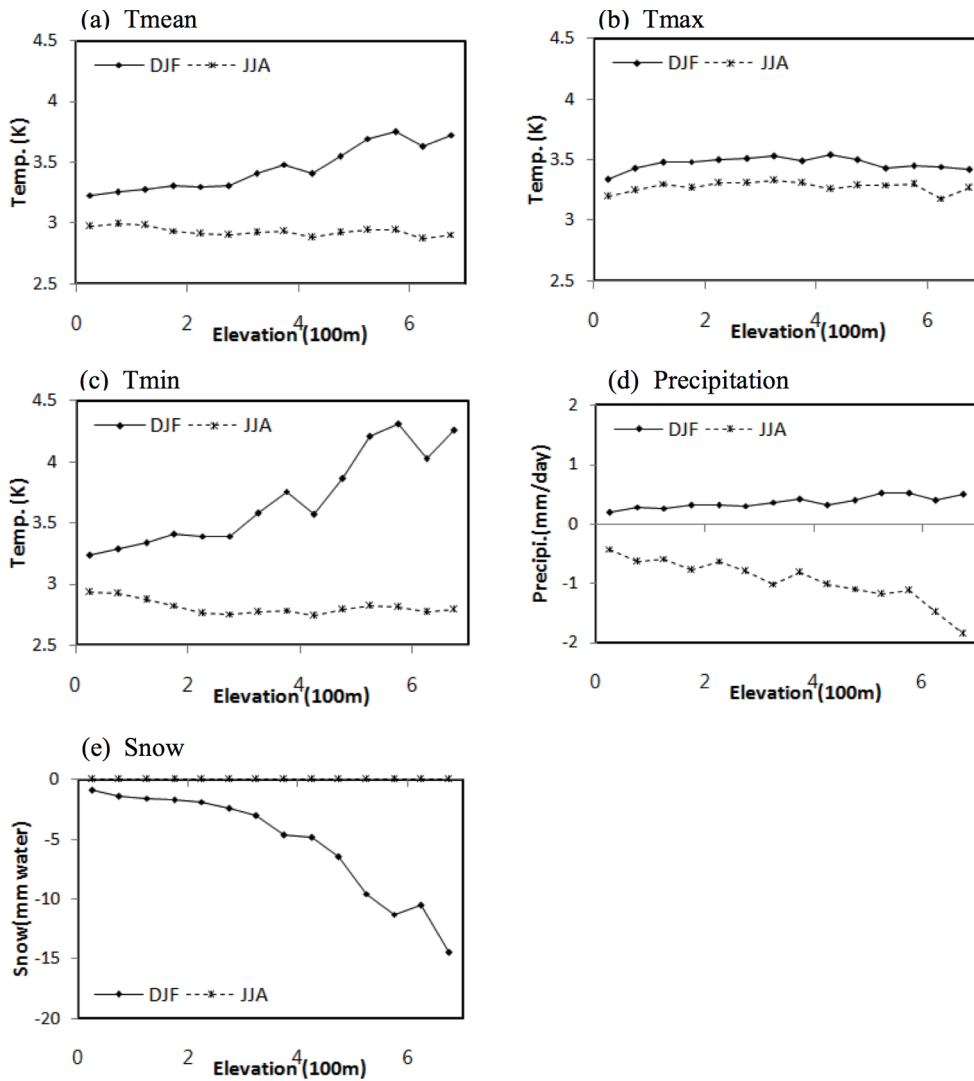


Fig. 6. Difference between the future (2071–2100) and reference (1971–2000) simulations in mean, maximum, and minimum temperature, precipitation, and snow amount as a function of elevation over Korea for the winter and summer seasons.

3.2 Projection of future climate simulation (2071–2100)

Figure 6 shows the elevation dependency of T_{mean} , T_{max} , T_{min} , precipitation, and snow changes (difference between 2071–2100 and 1971–2000) over Korea for the winter and summer seasons. The elevation categories are divided into 50 m intervals up to 700 m (x axis in Fig. 6), and the results are averaged over all grid points in each elevation category. As expected, all temperature fields show considerable warming (more than 2.5 K) in response to emission forcing (A1B), which is in line with previous climate change studies over Korea

(Im et al. 2007a, 2009; Im and Kwon 2007). Interesting point is that this warming is quite inhomogeneous in various respects. We first notice that the temperature change shows different seasonal responses along the elevation. While little relationship between the elevation and temperature (T_{mean} , T_{max} , and T_{min}) is shown for the summer season, the elevation dependency of T_{mean} and T_{min} is apparent for the winter. In particular, the degree of warming in winter T_{min} sharply accelerated with elevation, with maximum warming reaching above 4 K. The differential rate of seasonal warming could be explained by the snow-albedo feedback mechanism.

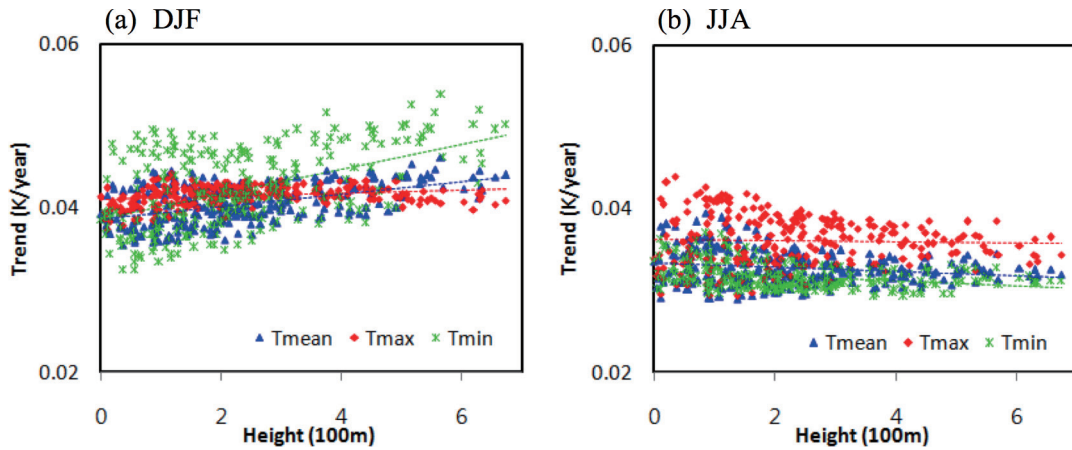


Fig. 7. Scatter plots of the altitudes (x-axis) against the T_{mean} , T_{max} , and T_{min} trend magnitude (y-axis: 2001–2100, K/year) from 248 grid points of nested domain simulation for the (a) winter and (b) summer.

For winter, change of T_{min} with elevation seems to be a mirror of snow behavior (correlation coefficient -0.96). This significant decrease of snow amount at high elevations under warming could lead to increased absorption of solar radiation (not shown) due to reduced surface albedo; this, in turn, would amplify further warming. Quantitatively, the reason for relatively less warming in the summer season could be partially associated with the free from snow, as well. Besides seasonal variations, the asymmetric behavior between T_{max} and T_{min} is relevant, which leads to a change of diurnal temperature range. Based on this projection, the decrease in the diurnal temperature range is larger at high elevations than at lower elevations during winter. Such asymmetric changes in T_{max} and T_{min} have been reported for other regions (Karl et al. 1993; Weber et al. 1994; Jungo and Beniston 2001). The possible cause of less elevation effect on T_{max} is that, even in the winter season at high elevation, T_{max} is mostly above 0 K (1971–2000: Fig. 2a) and 2 K (2071–2100: not shown); this warmer condition could not effectively work with relation to the snow formation and melting.

A continuous long-term simulation allows us to derive meaningful statistics regarding temporal evolution characteristic. Figure 7 presents the elevation distribution of the trend magnitude calculated from 248 grid points of nested domain simulation for the future 100-year period (2001–2100). Trend magnitudes are determined by the coefficient of the slope of an ordinary least squares regression line. For winter, the scatter plots of trend magnitude versus altitude again confirm a noticeable differential rate of warming between T_{max} and T_{min}

along the elevations, showing a faster warming rate of T_{min} at high elevation, in spite of larger scatter. On the other hand, the trends of summer temperature change do not reveal any relationship to the elevation, showing consistency with Fig. 6.

Next, the seasonal behavior of the precipitation change shows an opposite response along the elevation, with an increase in winter and a decrease in summer. Increased precipitation in the winter season is due to increased atmospheric moisture content (based on the Clausius-Clapeyron relation) rather than changes in large-scale circulation. Warmer temperatures lead to higher freezing levels; therefore, rainfall tends to increase while snowfall generally decreases. The change of summer precipitation also shows an elevation magnification effect, however the reduced precipitation is not associated with topographical modulation. Rather, it is tied to a decrease in precipitation in the ECHAM5-MPI/OM projection used as the initial and boundary forcing for the RegCM3 downscaling system. The downscaled results (both nested and mother domain) tend to follow the general pattern of ECHAM5-MPI/OM projection even though they exhibit a much greater fine scale structure reflecting the local response. When looking at the regional average over East Asia, including the Korean peninsula (100–150E, 20–50N), the ECHAM5-MPI/OM projects increases in precipitation for the twenty-first century (2071–2100) with respect to the reference simulation (1971–2000) (DJF: 8.2% and JJA: 6.6%, not shown), which is consistent with the GCMs ensemble projection reported by IPCC (2007). However, a detailed spatial structure could be diverse

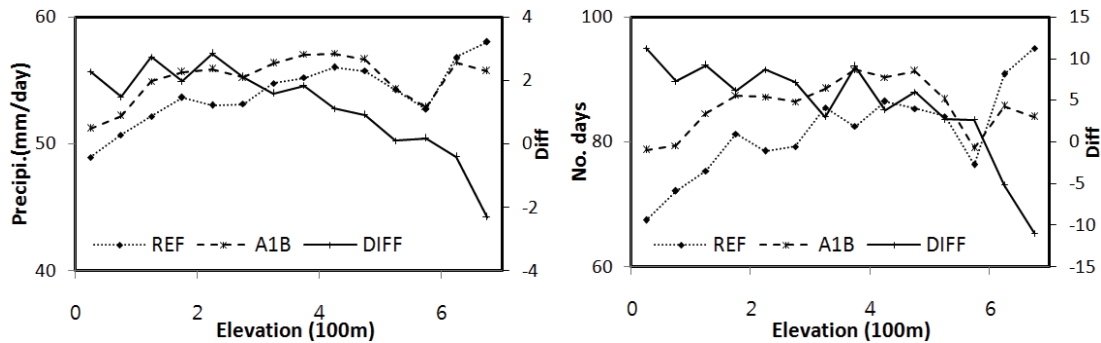


Fig. 8. Mean precipitation above the 95th percentile (left panel) and total number of days with precipitation above 80 mm intensity (right panel) of the reference (1971–2000) and future (2071–2100) simulations and their differences as a function of elevation over Korea.

and the ECHAM5-MPI/OM projected reduced summer precipitation over Korea, which is rather different from all ensemble average participating in the CMIP3 A1B projections. In fact, there is a large possibility of misinterpretation in deriving any consensus about precipitation change from the GCM projections over a narrow peninsula such as Korea. In this regard, we do not intend to confirm the quantitative assessment of future climate condition, but more simply, we aim at investigating the potential behavior in response to emission forcing. Note that a decrease in total precipitation does not proportionally contribute to a decrease in precipitation extremes. Figure 8 shows the elevation dependency of the mean precipitation exceeding the climatological 95th percentile precipitation and the total number of days in which the daily precipitation is greater than 80 mm. The former measures the change of extreme precipitation intensity while the latter measures the frequency of heavy precipitation. Even though total precipitation decreases regardless of elevation (Fig. 6d), both intensity and frequency of extreme precipitation tend to increase under warming, except for above 600 m. It implies an enhancement of relatively high intensity precipitation and a reduction of weak intensity precipitation as reported by other climate change studies (e.g., Kimoto et al. 2005; Kitoh et al. 2005; Kripalani et al. 2007). A sudden drop between 550–600 m is observed in both intensity and frequency pattern. Only two grid points are included in the height range of 550–600 m and it could bring biased results of the discontinuous variables such as precipitation.

To emphasize the topographical modulation of the surface climate change, we present the precipitation and snow for both the reference (1971–2000) and future (2071–2100) periods, together with the differences

between the periods along the south-north transects (128.5E, 35.5–38N) (Fig. 9). Snow is displayed for winter while precipitation is displayed for summer, considering the relevant change in the individual variable. We also provide the elevation transect used for simulations with 20 km grid spacing (black solid lines in Fig. 9) to facilitate the topographic role in the simulation. Note that the topography of the 20 km nested domain does not fully resolve the fluctuating feature of elevation, as observed in the 2-minute resolution global dataset produced by the United States Geological Survey (USGS, not shown). Even the elevation transect of the mother domain (60 km) is much more smooth, only reaching the maximum elevation at less than 400 m (not shown).

First of all, the precipitation and snow directly reflect the topographical signature, showing an apparent correlation with elevation. The climate sensitivity in response to emission forcing is different along the elevation, i.e., the change signal is more pronounced at higher elevation sites than at lower elevations. As for the snow change, some high percentages of change amounts are found in low elevation regions (right lower panel in Fig. 9). However it looks inflated in percentage sense because the absolute amount is very small. Topographically modulated patterns in precipitation are clearly shown in both the absolute values and in the change of percentages with respect to the reference simulation.

Such detailed information may have important implications for the design of adaptation measures for climate changes over a certain region, particularly regions like South Korea having complicated geographical features. For example, a different reduction ratio of absolute snow amounts between high mountain ridges and flat areas could lead to a totally different hydrological cycle in the future. In particular, when they link to

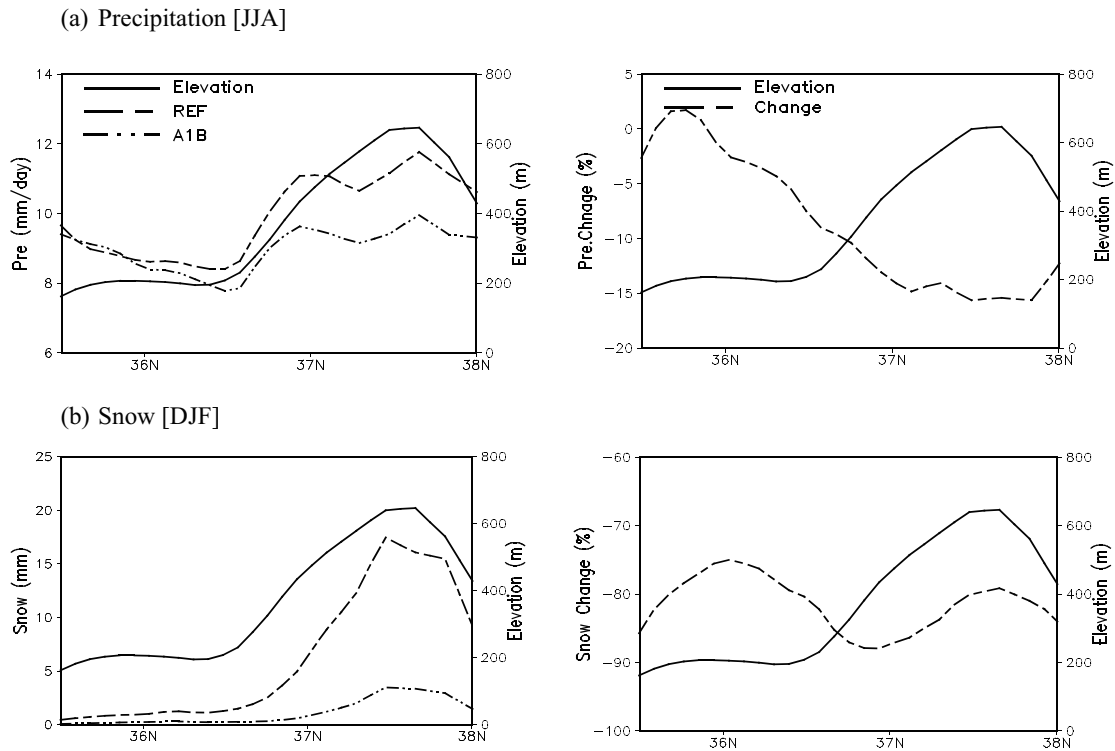


Fig. 9. Summer precipitation (a) and winter snow (b), and surface elevation along south-north transects (Longitude = 128.5E) from the reference and future (REF: 1971–2000 and A1B: 2071–2100, left panels) and their changes (right panels).

hydrological impact assessment studies, their influence could become larger, thus deriving completely different conclusions of climate change impact. In fact, Im et al. (2010b) reported that the changes in temperature and precipitation cause relatively large differences in runoff simulation for the Korean river basin. Even if these are just illustrative examples, they clearly show that a high resolution, by a more refined representation of topography, can improve the simulation of the hydrological cycle.

4. Summary and discussion

In this study, we presented an analysis of the elevation dependency of the present-day climate and future change from a high resolution regional climate projection (20 km). For fine-scale climate information over Korea, we performed dynamical downscaling of the ECHAM5/MPI-OM A1B scenario covering the period 1971–2100 (130-year) using a RegCM3 double-nested system. Validation of the present-day climate (1971–2000) against ASOS and ASOS+AWS dataset and the projection of future climate change were discussed with

a focus on the elevation dependency.

A strong elevation dependency of the surface climate variables is found for both the simulation and the observations. Temperature (T_{mean} , T_{max} , and T_{min}) clearly decreases with elevation regardless of season as is known from various observations (e.g., Barry 2008) while only the summer precipitation shows statistically significant relationship with elevation. The simulated temperature and precipitation reasonably capture the observed characteristics, showing the different feature between low and high elevations. For in-depth analysis, it would require a much more dense station network including both low- and high-elevation sites.

According to the differences between the latter part of the twenty-first (2071–2100) and twentieth (1971–2000) century, the temperature is projected to increase across all elevations. The increase in T_{min} is above 4 K, at high elevations in winter. Interestingly, the detailed structure of the changes in T_{min} and T_{max} shows different behaviors, in terms of season and elevation. An asymmetric response between T_{min} and T_{max} is an important feature implying a change of diurnal temperature

range under warming. It may be influenced by several simultaneous mechanisms, such as snow-albedo feedback and cloud-radiation feedback (Liu et al. 2009). In this study, we demonstrate the warming amplification in cold climate regimes (e.g., high elevation) in relation to the snow-albedo feedback mechanism based on the strong relationship between snow and T_{\min} . Under warming, the total precipitation and extreme precipitation intensity and frequency also show seemingly elevation-dependent pattern. The advantage of the complex topography is confirmed by transect analysis. The precipitation and snow directly reflect the topographical signature in their climatology. The sensitivity in the response to emission forcing is more pronounced at high elevations than at lower elevations, highlighting the importance of topographic forcing in generating the characteristics of local climatology. Improved accuracy of regional climate projection could lead to an enhanced reliability of interpretation of the warming effect, especially when linking climate change information to impact assessment studies.

Considering the lack of fine-scale climate change projections over Korea, this study contributes to extend our understanding of the characteristics of the climate change signal over a topographically diverse region such as Korea, in spite of the large uncertainty sources.

Acknowledgements

The authors wish to thank the two anonymous reviewers whose valuable comments and suggestions greatly improved the quality of this paper. We extend our thanks to Ms. Jina Hu for the analysis of the AWS data. This work was supported by the Korea Meteorological Administration Research and Development Program under Grant CATER 2009-1146 and Grant RACS 2010-4012. This work was also partially supported by the “Hydrometeorology research for the test-bed region” of National Institute of Meteorological Research (NIMR) funded by the Korea Meteorological Administration (KMA).

References

- Barry, R. G., 2008: *Mountain weather and climate* (3rd ed.), Cambridge University Press, Cambridge, 506 pp.
- Beniston, M., 2003: Climatic change in mountain regions: A review of possible impacts. *Climatic Change*, **59**, 5–31.
- Beniston, M., H. F. Diaz, and R. S. Bradley, 1997: Climatic change at high elevation sites: An overview. *Climatic Change*, **36**, 233–251.
- Fyfe, J. C., and G. M. Flato, 1999: Enhanced climate change and its detection over the Rocky Mountains. *J. Climate*, **12**, 230–243.
- Giorgi, F., J. W. Hurrell, M. R. Marinucci, and M. Beniston, 1997: Elevation dependency of the surface climate change signal: A model study. *J. Climate*, **10**, 288–296.
- Hagemann, S., H. Göttele, D. Jacob, P. Lorenz, and E. Roeckner, 2009: Improved regional scale processes reflected in projected hydrological changes over large European catchments. *Climate Dynamics*, **32**, 767–781.
- Im, E.-S., and W.-T. Kwon, 2007: Characteristics of extreme climate sequences over Korea using a regional climate change scenario. *Sci. Online Lett. Atmos.*, **3**, 17–20.
- Im, E.-S., E.-H. Park, W.-T. Kwon, and F. Giorgi, 2006: Present climate simulation over Korea with a regional climate model using a one-way double-nested system. *Theor. Appl. Climatol.*, **86**, 187–200.
- Im, E.-S., E. Coppola, F. Giorgi, and X. Bi, 2010a: Local effects of climate change over the Alpine region: A study with a high resolution regional climate model with a surrogate climate change scenario. *Geophys. Res. Lett.*, DOI 10.1029/2009GL041801, in press.
- Im, E.-S., I.-W. Jung, and D.-H. Bae, 2011: The temporal and spatial structure of recent and future trends in extreme indices over Korea from a regional climate projection. *Int. J. Climatol.*, **31**, 72–86.
- Im, E.-S., I.-W. Jung, H. Chang, D.-H. Bae, and W.-T. Kwon, 2010b: Hydrometeorological response to dynamically downscaled climate change simulations for Korean basins. *Climatic Change*, **100**, 485–508.
- Im, E.-S., M.-H. Kim, W.-T. Kwon, and S. Cocker, 2007a: Projected change in mean and extreme climate over Korea from a one-way double-nested regional climate model. *J. Meteorol. Soc. Japan*, **85**, 717–732.
- Im, E.-S., W.-T. Kwon, J.-B. Ahn, and F. Giorgi, 2007b: Multi-decadal scenario simulation over Korea using a one-way double-nested regional climate model system. Part 1: recent climate simulation (1971–2000). *Climate Dynamics*, **28**, 759–780.
- IPCC 2007. Climate Change 2007: The Physical Science Basis. Contribution of Working Group I to the Fourth Assessment Report of the Intergovernmental Panel on Climate Change. Solomon, S., D. Qin, M. Manning, Z. Chen, M. Marquis, K. B. Averyt, M. Tignor and H. L. Miller (eds). Cambridge Univ. Press, 996 pp.
- Jungo, P., and M. Beniston, 2001: Changes in the anomalies of extreme temperature anomalies in the 20th century at Swiss climatological stations located at different latitudes and altitudes. *Theoretical and Applied Climatol.*, **69**, 1–12.
- Karl, T. R., and coauthors, 1993: A new perspective on recent global warming: Asymmetric trends of daily maximum and minimum temperature. *Bull. Amer. Meteorol.*

- rol. Soc.*, **74**, 1007–1023.
- Kim, J., T. K. Kim, R. W. Arritt, and N. L. Miller, 2002: Impacts of increased atmospheric CO₂ on the hydroclimate of the Western United States. *J. Climate*, **15**, 1926–1942.
- Kim, J., 2001: A nested modeling study of elevation-dependent climate change signals in California induced by increased atmospheric CO₂. *Geophys. Res. Lett.*, **28**, 2951–2954.
- Kimoto, M., N. Yasutomi, C. Yokoyama, and S. Emori, 2005: Projected changes in precipitation characteristics around Japan under global warming. *Sci. Online Lett. Atmos.*, **1**, 85–88.
- Kitoh, A., M. Hosaka, Y. Adachi, and K. Kamiguchi, 2005: Future projections of precipitation characteristics in East Asia simulated by the MRI CGCM2. *Adv. Atmos. Sci.*, **22**, 467–478.
- Kripalani, R. H., J. H. Oh, and H. S. Chaudhari, 2007: Response of the East Asian summer monsoon to doubled atmospheric CO₂: Coupled climate model simulations and projections under IPCC AR4. *Theor. Appl. Climatol.*, **87**, 1–28.
- Leung, L. R., and S. J. Ghan, 1999: Pacific Northwest climate sensitivity simulated by a regional climate model driven by a GCM. Part II: 2×CO₂ simulations. *J. Climate*, **12**, 2031–2053.
- Liu, X., Z. Cheng, L. Yan, and Z. Y. Yin, 2009: Elevation dependency of recent and future minimum temperature surface air temperature trends in the Tibetan Plateau and its surroundings. *Global and Planetary Change*, **68**, 164–174.
- Qian, Y., S. J. Ghan, and L. R. Leung, 2009: Downscaling hydroclimatic changes over the Western US based on CAM subgrid scheme and WRF regional climate simulations. *Int. J. Climatol.*, in press.
- Sasaki, H., and K. Kurihara, 2008: Relationship between precipitation and elevation in the present climate reproduced by the non-hydrostatic regional climate model. *SOLA*, **4**, 109–112.
- Weber, R. O., P. Talkner, and G. Stefanicki, 1994: Asymmetric diurnal temperature change in the Alpine region. *Geophys. Res. Lett.*, **35**, L14701, doi:10.1029/2008GL034026.